



**Microbial rhamnolipid production in wheat straw hydrolysate supplemented with basic salts**

Journal:	<i>RSC Advances</i>
Manuscript ID:	RA-ART-04-2015-005800.R1
Article Type:	Paper
Date Submitted by the Author:	01-Jun-2015
Complete List of Authors:	Prabu, Rajagopalan; Hindustan Petroleum Green R&D Centre Bangalore, India, Kuila, Arindam; Hindustan Petroleum Green R&D Centre Bangalore, India, Ravishankar, Raman; Hindustan Petroleum Green R&D Centre Bangalore, India, Rao, Peddy; Hindustan Petroleum Green R&D Centre Bangalore, India, Choudary, Nettem; Hindustan Petroleum Green R&D Centre Bangalore, India, Velankar, Harshad; Hindustan Petroleum Green R&D Centre,

1 **Microbial rhamnolipid production in wheat straw hydrolysate supplemented with basic**  
2 **salts**

3 **Rajagopalan Prabu, Arindam Kuila, Raman Ravishankar, Peddy VC Rao, Nettem V**

4 **Choudary and Harshad Velankar\***

5 Hindustan Petroleum Green R & D Centre (HPGRDC), KIADB Industrial Area, Tarabahalli,  
6 Devenagundi, Hoskote, Bengaluru- 560067

7

8

9

10

11

12

13

14

15

16

17

18

19

20

21

22 **\*Correspondence Address:**

23 Email: [harshadv@hpcl.co.in](mailto:harshadv@hpcl.co.in)

24 Phone: 91-80- 28078580

25 Fax: 91-80-28078510

26 **Abstract**

27 Rhamnolipids are important glycolipids that find applications in the areas of crude oil  
28 bioremediation, enhanced oil recovery, food and pharmaceutical applications. The economic  
29 feasibility of rhamnolipid production mainly depends upon the cost of the substrate.  
30 Lignocellulosic biomass is a potential substrate for the production of several microbial  
31 metabolites and can also be used for rhamnolipid production. For the utilization of sugars  
32 from lignocellulosic biomass, the polymeric carbohydrates need to be hydrolysed for  
33 releasing the fermentable sugars for rhamnolipid production. In this study, pretreatment of  
34 wheat straw was carried out using sulphuric acid, phosphoric acid and ammonia. All the  
35 pretreated substrates were subjected to enzymatic hydrolysis using cellulases, produced by  
36 *Trichoderma reesei* NCIM 1186. Maximum reducing sugar yield (509.33 mg/g dry pretreated  
37 substrate) was obtained in case of biomass treated with 0.2% sulphuric acid at 150 °C for 15  
38 min which was further used for rhamnolipid production by *Pseudomonas aeruginosa* NCIM  
39 2036. The highest rhamnolipid production of 9.38 g/L was obtained in sugar hydrolysate  
40 (mainly containing cellobiose) supplemented with MgSO<sub>4</sub>, Na<sub>2</sub>HPO<sub>4</sub>, FeSO<sub>4</sub> and NaNO<sub>3</sub>.  
41 The production of rhamnolipid by *P. aeruginosa* NCIM 2036 using pure cellobiose as the  
42 sole carbon source was demonstrated. The current study showed that lignocellulosic biomass  
43 can be used as an alternative cost-effective substrate for rhamnolipid production.

44

45 **Keywords:** Rhamnolipid, *Pseudomonas aeruginosa*, wheat straw, cellobiose, nutrients

## 46 1. Introduction

47 The use of microbial biosurfactants as alternatives to chemical surfactants has gained  
48 considerable attention owing to their ability to solubilize hydrocarbons.<sup>1</sup> Biosurfactants  
49 consist of the hydrophobic and hydrophilic groups that confer them the property to  
50 accumulate between fluid phases, thereby reducing surface and interfacial tension.<sup>2</sup> In  
51 addition, biosurfactants are biodegradable and less toxic than chemical surfactants and retain  
52 activity under wide ranges of temperatures, pH and salinity.<sup>3</sup> Due to several advantageous  
53 features, biosurfactants can be used for diverse applications such as enhanced oil recovery,  
54 oil spill clean-up, emulsification, wetting, foaming, and cleansing.<sup>4,5</sup> The use of microbial  
55 biosurfactants during the enzymatic hydrolysis of biomass was found to be beneficial in  
56 increasing the reducing sugar yields.<sup>6</sup> Moreover, the addition of rhamnolipids to cultures of  
57 *Penicillium expansum* increased the production of cellulolytic enzymes.<sup>7</sup>

58 Biosurfactant properties (structural and chemical) and production is greatly influenced  
59 by the choice of microorganism, substrate and process conditions.<sup>8</sup> Among different  
60 biosurfactants, rhamnolipids produced by different strains of *Pseudomonas* sp. have been  
61 studied extensively.<sup>9</sup> Chavez and Maier<sup>9</sup> mentioned that the production of rhamnolipids by  
62 *Pseudomonas* usually occurred at the onset of stationary phase and high rhamnolipid yields  
63 were obtained during fed batch cultivations. Several substrates of synthetic or natural origin  
64 and even industrial wastes have been used to produce rhamnolipids.<sup>10</sup> Recently, rhamnolipid  
65 produced from a synthetic substrate (glycerol), albeit at lower concentrations of 1.62 g/L, by  
66 a genetically engineered strain of *Pseudomonas aeruginosa*, was used for enhanced crude oil  
67 recovery in simulated oil reservoirs.<sup>11</sup> Another report indicated that crude oil itself could be  
68 used as a naturally occurring carbon source for rhamnolipid production, although the reported  
69 concentrations (20 mg/L) were lower.<sup>12</sup> Higher rhamnolipid concentrations of 13.93 g/L were  
70 produced by *Pseudomonas* SWP-4 with waste cooking oil as the substrate.<sup>13</sup>

71 Although the waste streams are inexpensive, they are less preferred for rhamnolipid  
72 production due to their non-uniform compositions and dilute nature leading to inconsistent  
73 product formation.<sup>10</sup>

74 Due to their cheaper cost and abundant availability, lignocellulosic biomass can be  
75 used as an inexpensive feedstock for rhamnolipid production. The use of biomass would  
76 however include the unlocking of fermentable carbohydrates by thermochemical pre-  
77 treatment followed by enzymatic hydrolysis.<sup>3,14</sup> The selection of suitable thermochemical  
78 methods for biomass pretreatment is critical to improve the fermentability of sugar  
79 hydrolysates. The dilute acid process has been widely used for the pretreatment of various  
80 biomass varieties. The sugar hydrolysate generated via dilute acid hydrolysis has been found  
81 to be fermentable for producing bioethanol, lipids, triacylglycerols etc.<sup>15,16</sup> In order to  
82 overcome nutrient deficiency of sugar hydrolysate, macro and micro nutrient  
83 supplementation has been tried for improving microbial product formation.<sup>17</sup> Earlier studies  
84 have indicated that magnesium, phosphorus, iron and nitrogen sources are important factors  
85 for microbial rhamnolipid production.<sup>18,19</sup> For cellobiose rich sugar hydrolysates, selection of  
86 microbial strains with beta-glucosidase (cellobiases) activities is essential to produce value  
87 added fermented products. Although, strains of *Pseudomonas* can utilize diverse  
88 carbohydrates, reports related to their cellobiose utilization are few, possibly due to lower  
89 cellobiase activities.<sup>20,21</sup>

90 In the present study, sugar hydrolysate generated after enzymatic hydrolysis of  
91 pretreated wheat straw was used for rhamnolipid production. The concentrations of nutrients  
92 ( $\text{MgSO}_4$ ,  $\text{Na}_2\text{HPO}_4$ ,  $\text{FeSO}_4$  and  $\text{NaNO}_3$ ) to be added to wheat straw hydrolysate were  
93 optimized using central composite design (CCD) based response surface methodology  
94 (RSM). The production of mono and di rhamnolipids was confirmed by Fourier transform  
95 infrared spectroscopy (FTIR) and nuclear magnetic resonance (NMR) spectroscopy.

## 96 2. Material Methods

### 97 2.1 Microbial growth and inoculum preparation

98 *Pseudomonas aeruginosa* NCIM-2036 (ATCC 19429) and *Trichoderma reesei* NCIM 1186  
99 (ATCC 26921) were procured from National Culture of Industrial Microorganisms (NCIM),  
100 Pune, India and both stored until use at 4 °C. *Pseudomonas* inoculum preparation was done  
101 by inoculating a loopful of culture from the slants into 10 ml sterile nutrient broth (Himedia)  
102 to obtain cell growth (O.D: 0.6 @ 600 nm) after incubation at 30 °C for 24 h. The cell  
103 suspension was used as inocula for fermentative rhamnolipid production. *Trichoderma*  
104 inoculum preparation was done by inoculating a loopful of culture from the slants onto a  
105 Potato Dextrose Agar (Himedia) slant and incubated at 30 °C for 72 h hours till visible  
106 growth was observed. Inoculum for cellulase production was prepared by scrapping spores  
107 from the slants into sterile water.

108

### 109 2.2 Enzyme production

110 Cellulase enzyme production was carried out as described by Das *et al.*<sup>22</sup> by culturing  
111 *Trichoderma reesei* NCIM 1186 under solid state fermentation (SSF). Medium preparation  
112 for SSF was carried out by mixing the autoclaved wheat bran with Czapek dox minimal  
113 media<sup>23</sup> at 1:1 (w/v) ratio and incubated for 96 h at 30 °C. On completion, the grown cultures  
114 were extracted with sterile distilled water in 1:2 (w/v) ratio. The liquid extract was  
115 centrifuged at 5,000 rpm, 4 °C for 10 min for removing insoluble material. The cellulase  
116 activity of the supernatant was determined as per the standard protocols.<sup>24,25</sup> The  
117 endoglucanase, exoglucanase and xylanase activities of the supernatant were found to be 25  
118 IU/gds, 7.29 IU/gds and 121.25 IU/gds, respectively. The supernatant was further used for  
119 enzymatic hydrolysis of pretreated wheat straw.

120

### 121 **2.3 Wheat straw**

122 Wheat straw (approx. avg. particle size of 0.5 mm) was procured from local sources around  
123 Bangalore, India and dried in an oven at 60 °C for 48-72 h, till a constant biomass weight was  
124 obtained.

125

### 126 **2.4 Thermochemical pretreatment**

127 Wheat straw pretreatment was carried out using 0.5% (v/v) sulphuric acid, 0.2% (v/v)  
128 phosphoric acid or 20% (v/v) ammonia at 150 °C for 15 min in a 500 mL PARR reactor.  
129 After every pretreatment, the biomass was washed with distilled water and dried overnight at  
130 60°C until constant biomass weight was obtained. The dried biomass was further used for  
131 enzymatic hydrolysis.

132

### 133 **2.5 Enzymatic hydrolysis of pretreated wheat straw**

134 To pretreated wheat straw, the required quantity of enzyme (18.67 FPU/g of dry pretreated  
135 biomass) was added to obtain solid loadings of 15% (w/v) and incubated at 50 °C for 24 h.  
136 After hydrolysis, samples were withdrawn and tested for reducing sugar concentrations by  
137 using an Ultra-High Pressure Liquid Chromatography (Agilent 1290 UHPLC) by the method  
138 described earlier.<sup>26</sup> The sugar-hydrolysate was used for rhamnolipid production.

139

### 140 **2.6 Cellobiose Utilization**

141 To determine rhamnolipid production from pure cellobiose, *Pseudomonas aeruginosa* NCIM  
142 2036 was cultured in LB medium<sup>27</sup> with cellobiose (7 g/L) (Himedia, India) as the sole  
143 carbon source and incubated at 32°C upto 72 hr. Samples were collected periodically and  
144 cellobiose utilization was determined by using an Ultra-High Pressure Liquid

145 Chromatography (Agilent 1290 UHPLC) by the method described earlier.<sup>26</sup> The production  
146 of rhamnolipid was determined by the orcinol method.

147

## 148 **2.7 Rhamnolipid fermentation**

149 200 mL sugar hydrolysate was inoculated with 1% (v/v) of 24 h old *Pseudomonas* sp. culture  
150 and incubated at 30 °C, 150 rpm for 72 h. Samples was periodically withdrawn and tested for  
151 microbial growth (dry weight basis method) and rhamnolipid production (Orcinol method).

152

## 153 **2.8 Optimization of rhamnolipid production**

154 Optimization of rhamnolipid production from *Pseudomonas* sp was carried out using CCD  
155 based RSM. Optimization of rhamnolipid production was carried out by varying following  
156 parameters MgSO<sub>4</sub> (143-333 ppm), Na<sub>2</sub>HPO<sub>4</sub> (5000-9000 ppm), FeSO<sub>4</sub> (30-90 ppm) and  
157 NaNO<sub>3</sub> (8000-10000 ppm). All experiments were carried out in triplicates. Table 1 shows the  
158 experimental design and response for rhamnolipid production. The experimental data were  
159 analyzed by the Response Surface Regression (RSREG) method to fit the second-order  
160 polynomial equation (SAS, 1990):

$$161 \quad Y = \beta_0 + \sum_{i=1}^5 \beta_i x_i + \sum_{i=1}^5 \beta_{ii} x_i^2 + \sum_{i=1}^4 \sum_{j=i+1}^5 \beta_{ij} x_i x_j \quad (1)$$

162 Where, Y is the response (rhamnolipid yield);  $\beta_0$ ,  $\beta_i$ ,  $\beta_{ii}$  and  $\beta_{ij}$  are constant coefficients  
163 and  $x_i$ ,  $x_j$  are the coded independent variables, which influence the response variables Y. This  
164 response is preferred because a relatively few experimental combinations of the variables are  
165 sufficient to estimate potentially complex response function.

166

## 167 **2.9 Recovery of Rhamnolipid**

168 Rhamnolipid extraction from wheat straw hydrolysate was carried out as per the method  
169 described by Zhi-Feng *et al.*<sup>28</sup> At regular intervals, samples were taken from the fermentation

170 media and the pH of the broth was adjusted to pH 8 by addition of 1.0 M NaOH and  
171 centrifuged at 13,756 rcf for 10 min. On centrifugation, the pH of the supernatant was  
172 readjusted to pH 2 by addition of 1.0 M HCl followed by extraction in cold ethyl acetate at a  
173 ratio of 1:5. After extraction, the solvent was evaporated using a Buchi Rotavap at 70 °C,  
174 120 mbar and the residue was used for further purification.

175

## 176 **2.10 Analysis**

### 177 **2.10.1 Orcinol method**

178 Rhamnolipid concentration was determined by the orcinol method as described by Rahman *et*  
179 *al.*<sup>29</sup> A standard curve was plotted using Rhamnose (Sigma) as the standard.

### 180 **2.10.2 Cell growth determination**

181 Growth of *Pseudomonas aeruginosa* during rhamnolipid production was determined by  
182 measuring culture densities, at 600 nm.

### 183 **2.10.3 Emulsification index test**

184 Emulsification index and interfacial tension (IFT) of rhamnolipid samples were determined  
185 by the method described by Noh *et al.*<sup>30</sup> and Christova *et al.*<sup>31</sup>, respectively.

### 186 **2.10.4 Preparative TLC**

187 For the separation of rhamnolipid from lignocellulosic hydrolysate, preparative TLC method  
188 was used.<sup>32</sup>

### 189 **2.10.5 FTIR measurements**

190 The Infrared spectra of the partially purified product were recorded using the JASCO FTIR  
191 instrument and the IR spectra are presented in % transmittance with respect to wave numbers  
192 ( $\text{cm}^{-1}$ ).

### 193 **2.10.6 NMR measurements**

194 The partially purified product was characterized by  $^1\text{H}$  NMR using Jeol 400 MHz NMR  
195 spectrometer.  $^1\text{H}$  NMR spectra were recorded using tetramethylsilane (TMS) as an internal  
196 standard.

197

### 198 **3. Results and Discussion**

#### 199 **3.1 Enzymatic hydrolysis of pretreated wheat straw**

200 The dilute acid pretreatment of lignocellulosic biomass causes effective removal of  
201 hemicellulose, making the residual biomass amenable to enzymatic hydrolysis.<sup>33,34</sup> In our  
202 previous study<sup>35</sup>, the optimum conditions for wheat straw pre-treatment were determined by  
203 subjecting the biomass to different (0.1-1%) acid (sulphuric and phosphoric) and ammonia  
204 (1-20%) concentrations for varying periods (5-120 min) and temperatures (120 °C-180 °C)  
205 (Data not shown). The pretreated biomass was subjected to enzymatic hydrolysis with  
206 *Trichoderma* cellulases at 50 °C for 24 h and the reducing sugar concentrations were  
207 measured. Dilute sulphuric acid as a catalyst for biomass treatment has been previously found  
208 to be effective for hydrolysis and suitable due to the requirement for milder operating  
209 conditions. Likewise, in the current study, the use of 0.2% sulphuric acid at 150 °C for 15  
210 min for wheat straw pretreatment resulted in maximum sugar yield of 509.33 mg/g of dry  
211 pretreated biomass (Data not shown) after 24 h of enzymatic hydrolysis and the sugar  
212 hydrolysate was used as the media for microbial rhamnolipid production.

213

#### 214 **3.2 Rhamnolipid production from pure cellobiose**

215 To confirm the utilization of cellobiose by the selected strain of *Pseudomonas aeruginosa*, the  
216 microorganism was cultured in minimal media containing cellobiose as the sole carbon  
217 source. After inoculation of the *Pseudomonas* sp. culture, a lag phase was observed till up to  
218 12 h, after which the cells started growing exponentially up till 48 h and later entered the

219 stationary phase. Rhamnolipid production was detected from the beginning of the exponential  
220 phase, reached maximum concentration of  $3.12 \pm 0.35$  g/L after 60 h of incubation and  
221 thereafter remained constant (Fig. 1). At the end of fermentation (72 h), approximately 30%  
222 (w/v) cellobiose remained unutilized in the medium.

223

### 224 **3.3 Rhamnolipid production in sugar hydrolysate**

225 The fermentation of sugar hydrolysate containing 98% (w/v) cellobiose, 1% (w/v) glucose  
226 and 1% (w/v) xylose by *Pseudomonas* sp. (without nutrient supplementation) results in lower  
227 ( $1.79 \pm 0.2$  g/L) rhamnolipid production. The lower rhamnolipid production in sugar  
228 hydrolysate can be attributed to the nutrient deficient conditions, which are essential for  
229 optimum microbial growth and metabolite formation.<sup>36,37</sup> For enhancing the fermentability of  
230 sugar hydrolysate, the optimum concentrations of selected micronutrients (magnesium and  
231 iron) and macronutrients (nitrogen and phosphorus) were determined through CCD based  
232 RSM.

233

### 234 **3.4 CCD based RSM for optimization of rhamnolipid production by *Pseudomonas*** 235 ***aeruginosa***

236 The design matrix of the variables in uncoded units along with response has been given in  
237 Table 1. Using the designed experimental data (Table 1), the second-order polynomial model  
238 for the rhamnolipid production is shown as follows:

$$\begin{aligned} 239 \text{ Rhamnolipid (g/L)} = & - 89.03 - 7.72 \times \text{MgSO}_4 - 2.38 \times \text{Na}_2\text{HPO}_4 + 0.07 \times \text{FeSO}_4 + 25.15 \times \\ 240 & \text{NaNO}_3 + 1.39 \times \text{MgSO}_4 \times \text{MgSO}_4 + 0.20 \times \text{Na}_2\text{HPO}_4 \times \text{Na}_2\text{HPO}_4 - 1.39 \times \text{NaNO}_3 \times \text{NaNO}_3 + \\ 241 & 0.07 \times \text{MgSO}_4 \times \text{MgSO}_4 + 0.03 \times \text{MgSO}_4 \times \text{NaNO}_3 - 0.06 \times \text{Na}_2\text{HPO}_4 \times \text{NaNO}_3 \quad (2) \end{aligned}$$

242 Based on the experimental response, runs 17 and 25 had the maximum and minimum  
243 rhamnolipid production, respectively. The ANOVA results of second-order response surface

244 models for rhamnolipid production have been given in Table 2. From ANOVA analysis of  
245 regression model, at 20 degree of freedom, F-value was 93.54 and p-value was <0.001. From  
246 the F and P values it indicated that the quadratic regression model for rhamnolipid production  
247 was significant. The 'goodness of fit' for the model was checked by the determination of  
248 coefficient ( $R^2$ ). The  $R^2$  value provided a measure of the variability in the actual response  
249 values that could be explained by the experimental factors and their interactions. A value of  
250 one represents the ideal case at which 100% of the variation in the observed value can be  
251 explained by the model. In this case, the mathematical model was found to be reliable with  $R^2$   
252 value of 98.72%, whereas, the adjusted  $R^2$  value of 97.66% indicated that only 2.34% of the  
253 total variations were not explained by the model.

254 The 3D response surface plots represent the regression equation. Figures 2, 3 and 4 represent  
255 the 3D response surface plots for the optimum conditions of rhamnolipid production. Each  
256 figure represents the effect of two variables on rhamnolipid production. Fig. 2 indicates that  
257 maximum rhamnolipid production of 9.45 g/L was obtained on addition of 90 ppm  $\text{FeSO}_4$   
258 and 8760 ppm  $\text{NaNO}_3$ . Fig. 3 depicts that the maximum rhamnolipid levels were attained at  
259 143 ppm of  $\text{MgSO}_4$  and 8760 ppm of  $\text{NaNO}_3$ . Fig. 4 similarly shows the effect of varying  
260  $\text{MgSO}_4$  and  $\text{FeSO}_4$  concentrations on rhamnolipid production. Overall, the supplementation  
261 of hydrolysate with 143 ppm of  $\text{MgSO}_4$ , and 90 ppm of  $\text{FeSO}_4$  (micronutrients) and 9000  
262 ppm of  $\text{Na}_2\text{HPO}_4$  and 8760 ppm of  $\text{NaNO}_3$  resulted in maximum rhamnolipid production.  
263 Under optimized conditions (with nutrient supplementation) the maximum predicted product  
264 concentration of 9.45 g/L was similar to the experimental response (9.38 g/L). At the end of  
265 fermentation, around 48% (w/v) of the initial sugars remained unutilized. The Liquid  
266 hydrolysate containing about 76 g/L of reducing sugars (initial) produced 9.43 g/L of  
267 rhamnolipid by utilizing 39.52 g/L of reducing sugars. The unutilized sugars remained in the  
268 media was about 36.48 g/L.

### 269 **3.5 *Pseudomonas* cell growth in sugar hydrolysate**

270 The growth of *Pseudomonas aeruginosa* in sugar hydrolysate supplemented with macro and  
271 micro nutrients was determined (Fig. 5). After inoculation, the cells continued to grow  
272 steadily till the 24<sup>th</sup> hour of incubation, beyond which the increase in cell mass remained  
273 relatively constant. The rhamnolipid production was initiated after the 12<sup>th</sup> hour of  
274 inoculation and attained maximum levels by the 68<sup>th</sup> hour of incubation. The maximum  
275 biomass (0.912 OD<sub>600</sub>) and rhamnolipid (9.35 g/L) concentrations were attained after 72 h of  
276 incubation. It was observed that rhamnolipid production was initiated during the mid  
277 exponential phase of *Pseudomonas* cell growth and continued to rise even after the cells had  
278 attained the stationary phase.

279 In the present study, rhamnolipid concentrations obtained in sugar hydrolysate were  
280 marginally higher than the previously reported levels of 6 g/L, 4 g/L and 6.6 g/L in synthetic  
281 media containing glucose, mannitol or sunflower oil respectively.<sup>38,39,40</sup>

282

### 283 **3.6 Rhamnolipid characterization**

#### 284 **3.6.1 Emulsification index and interfacial tension**

285 The rhamnolipids produced by *P. aeruginosa* in sugar hydrolysate reduced the culture  
286 medium surface tension to values around 3 mN/m, with emulsifying indexes of 56 % against  
287 64% for CTAB (chemical surfactant).

288

#### 289 **3.6.2 Fourier Transform Infrared Spectroscopy (FTIR) studies of the partially purified** 290 **product**

291 The FTIR spectrum of the partially purified product is present in Table 3. The IR bands  
292 could be assigned to frequencies due to C-C stretching of SP<sup>3</sup> and SP<sup>2</sup> carbons, C-H,  
293 Carbonyl groups from esters, pyrnal (oxygen in six-membered ring) groups, C-O groups

294 present in the rhamnolipid product. The assignments of the major IR bands observed over the  
295 product have been tabulated (Table 3). The presence of C-C, C-H, C-O, C=O, RCOO-, C-O-  
296 (ring) were confirmed. Similar observations were previously reported by Rahman *et al.*<sup>41</sup>  
297 Therefore, FTIR analysis indicated the presence of mono and di rhamnolipids in the extracted  
298 sample.

299

### 300 3.6.3 Characterization of the partially purified product by <sup>1</sup>H NMR

301 The <sup>1</sup>H NMR spectrum of the partially purified product is presented in Fig. 6. The  
302 following assignments are made based on the <sup>1</sup>H chemical shifts (Table 4). From the <sup>1</sup>H  
303 NMR data, the chemical shifts could be assigned to different protons of the functional groups  
304 present in the rhamnolipids. The <sup>1</sup>H NMR spectrum indicated that the sample predominantly  
305 contained mono-rhamnolipids along with di-rhamnolipids. These NMR observations are in  
306 agreement with the earlier report.<sup>42</sup>

307 The peaks reported in the literature for a mixture of mono and di-rhamnolipids ranging  
308 from 7 – 9 ppm were attributed to the –CH<sub>2</sub>-CH- linkage (region III).<sup>39</sup> The NMR spectrum  
309 in the range 7-8 ppm observed in the present study could be attributed to the presence of  
310 mono-rhamnolipids predominantly. Nevertheless, the di-rhamnolipid also has –CH<sub>2</sub>-CH-  
311 linkage which could overlap in the same chemical shift region. In the present study, there are  
312 very negligible peaks between the ranges 8 – 9 ppm. The signals between 7-8 ppm were  
313 assigned specifically to mono-rhamnolipid and the rest of the signals (8-9 ppm) were  
314 attributed to di-rhamnolipid.<sup>42</sup> However in the present study, it could be observed in the Table  
315 4 that the absence of peaks or very weak NMR signals in the range 8 to 9 ppm indicated the  
316 presence of di-rhamnolipid in lesser quantities (region III).

317 Therefore, from the <sup>1</sup>H NMR spectra, it could be concluded that the partially purified  
318 product contained mono-rhamnolipids in predominance and lesser quantities of di-

319 rhamnolipids.

320

#### 321 **4. Conclusion**

322 The present study showed for the first time, the successful production of microbial  
323 rhamnolipids in lignocellulosic sugar hydrolysate. The fermentability of hydrolysate was  
324 improved by the addition of selected nutritional supplements at specific concentrations. The  
325 rhamnolipid concentrations obtained in our study were comparable to the reported levels  
326 obtained using relatively expensive substrates.

327

#### 328 **Acknowledgement**

329 Authors thank Mrs. Kusum Kumari Vsiwakarma for her support in biosurfactant analysis.  
330 The authors acknowledge Hindustan Petroleum Green Research and Development Centre  
331 (HPGRDC), Bangalore, India for the financial support to conduct this research.

332

#### 333 **5. References**

- 334 1 R. S. Makkar and K. J. Rockne, *Environ. Toxicol. Chem.*, 2003, **22**, 2280-2292.
- 335 2 K. G. Sanket and B. N. Yagnik, *Asian J. Exp. Biol. Sci.*, 2013, **4**, 1-8.
- 336 3 R. S. Makkar, S. S. Cameotra and I. M. Banat, *AMB Exp.*, 2011, **1**, 5.
- 337 4 M. Pacwa-Płociniczak, G. A. Płaza, Z. Piotrowska-Seget and S. S. Cameotra, *Int. J.*  
338 *Mol. Sci.*, 2011, **12**, 633-654.
- 339 5 E. Shoeb, F. Akhlaq, U. Badar, J. Akhter and S. Imtiaz, *Acad. Res. Int.*, 2013, **4**, 243-  
340 252.
- 341 6 Y. Feng, J. Jiang, L. Zhu, L. Yue, J. Zhang and S. Han, *Biotechnol. Biofuels*, 2013, **6**,  
342 161.

- 343 7 H. Y. Wang, B. Q. Fan, C. H. Li, S. Liu and M. Li, *Bioresource Technol.*, 2011, **102**,  
344 6515-6521.
- 345 8 R. Reis, G. J. Pacheco, A. G. Pereira and D. M. G. Freire, in *Biodegradation-Life of*  
346 *Science*, ed. R. Chamy and F. Rosenkranz, New York: InTech, 2013, ch. 2, pp. 31-61.
- 347 9 G. S. Chavez and R. M. Maier, in *Biosurfactants Microbiology Monographs*, ed. G. S.  
348 Chavez, Springer-Verlag: Berlin, Germany, 2011, vol. 20, pp. 1-11.
- 349 10 M. Henkel, M. M. Müller, J. H. Kügler, R. B. Lovaglio, J. Contiero, C. Syldatk and R.  
350 Hausmann, *Proc. Biochem.*, 2012, **47**, 1207-1219.
- 351 11 F. Zhao, R. Shi, J. Zhao, G. Li, X. Bai, S. Han and Y. Zhang, *J. Appl. Microbiol.*,  
352 2015, **118**, 379-389.
- 353 12 E. Antoniou, S. Fodelianakis, E. Korkakaki and N. Kalogerakis, *Front. Microbiol.*,  
354 2015, **6**, 274.
- 355 13 G. Lan, Q. Fan, Y. Liu, C. Chen, G. Li, Y. Liu and X. Yin, *Biochem. Eng. J.*, 2015,  
356 **101**, 44-54.
- 357 14 Q. Shao, S. P. S. Chundawat, C. Krishnan, B. Bals, L. C. Sousa, K. D. Thelen, B. E.  
358 Dale and V. Balan, *Biotechnol. Biofuels*, 2010, **3**, 12.
- 359 15 Q. Wang, Q. Zhu, J. Xu and J. Sun, *BioResources*, 2014, **9**, 6841-6850.
- 360 16 Z. Ruan, M. Zanotti, Y. Zhong, W. Liao, C. Ducey and Y. Liu, *Biotechnol. Bioeng.*,  
361 2013, **110**, 1039-1049.
- 362 17 S. P. S. Chundawat, G. T. Beckham, M. E. Himmel and B. E. Dale, *Annu. Rev. Chem.*  
363 *Biomol. Eng.*, 2011, **2**, 121-145.
- 364 18 Z. Luo, X. Z. Yuan, H. Zhong, G. M. Zeng, Z. F. Liu, X. L. Ma, and Y. J. Zhu, *Cent.*  
365 *South Univ.*, 2013, **20**, 1015-1021.
- 366 19 S. Mehdi, J. S. Dondapati and P. K. S. M. Rahman, *Biotechnology*, 2011, **10**, 183-  
367 189.

- 368 20 C. L. Cheng and J. S. Chang, *Bioresource Technol.*, 2011, **102**, 8628-8634.
- 369 21 R. Tiwari, S. Singh, P. Shukla and L. Nain, *RSC Adv.*, 2014, **4**, 58108-58115.
- 370 22 M. Das, R. Banerjee and S. Bal, *Braz. Arch. Biol. Technol.*, 2008, **51**, 35-41.
- 371 23 N. Pensupa, M. Jin, M. Kokolski, D. B. Archer and C. Du, *Bioresource Technol.*, 213,  
372 **149**, 261-267.
- 373 24 T. W. Jeffries, W. W. Yang and M. W. Davis, *Appl. Biochem. Biotechnol.*, 1998, **70-**  
374 **72**, 257-265.
- 375 25 Q. Zhang, C. M. Lo and L.K. Ju, *Bioresource Technol.*, 2007, **98**, 753-760.
- 376 26 R. C. Kuhad, R. Gupta, Y. P. Khasa and A. Singh, *Bioresource Technol.*, 2010, **101**,  
377 8348-8354.
- 378 27 H. Kahraman and S. O. Erenler, *Prikl. Biokhim. Microbiol.*, 2012, **48**, 212-217.
- 379 28 L. Zhi-Feng, Z. Guang-Ming, Z. Hua, Y. Xing-Zhong, F. Hai-Yan, Z. Mei-Fang, M.  
380 Xiao-Ling, L. Hui and L. Jian-Bing, *World J. Microbiol. Biotechnol.*, 2012, **28**, 175-  
381 181.
- 382 29 P. K. S. M. Rahman, G. Pasirayi, V. Auger and Z. Ali, *Biotechnol. Appl. Biochem.*,  
383 2010, **55**, 45-52.
- 384 30 N. A. M. Noh, A. A. A. Abdulah, M. N. M. Ibrahim and A. R. M. Yahya, *J. Gen.*  
385 *Appl. Microbiol.*, 2012, **58**, 153-161.
- 386 31 N. Christova, B. Tuleva, R. Cohenb, G. Ivanova, G. Stoevd, M. Stoilova-Disheva  
387 and I. Stoineva, *Z. Naturforsch. C.*, 2011, **66**, 394-402.
- 388 32 T. Janek, M. Lukaszewicz and A. Krasowska, *Colloids Surf. B Biointerfaces*, 2013,  
389 **110**, 379-386.
- 390 33 E. Déziel, F. Lépine, S. Milot and R. Villemur, *(BBA)-Mol. Cell Biol. L.*, 2000, **1485**,  
391 145-152.
- 392 34 Y. Sun and J. Cheng, *Bioresource Technol.*, 2002, **83**, 1-11.

- 393 35 A. Kuila, P. V. C. Rao, N. V. Choudary, S. Gandham and H. R. Velankar, *Environ.*  
394 *Prog. Sust. Energ.*, 2015, doi: 10.1002/ep.12102.
- 395 36 R. P. Chandra, R. Bura, W. E. Mabee, A. Berlin, X. Pan and J. N. Saddler, *Biofuels*,  
396 2007, **108**, 67-93.
- 397 37 H. Jørgensen, *Appl. Biochem. Biotechnol.*, 2009, **153**, 44-57.
- 398 38 E. Eldardiry, F. Hellal, H. Mansour and M. A. E. Hady, *Agric. Sci.*, 2013, **4**, 14-22.
- 399 39 S. Y. Chen, W. B. Lu, Y. H. Wei, W. M. Chen and J. S. Chang, *Biotechnol. Progr.*,  
400 2007, **23**, 661-666.
- 401 40 M. I. Maqsood, A. Jamal and H. A. Azeem, *Biologia*, 2011, **57**, 121-132.
- 402 41 P. K. S. M. Rahman, G. Pasirayi, V. Auger and Z. Ali, *Biotechnol. Appl. Biochem.*,  
403 2010, **55**, 45-52.
- 404 42 T. B. Lotfabad, H. Abassi, R. Ahmadkhaniha, R. Roostaazad, F. Masoomi, H. S.  
405 Zahiri, G. Ahmadian, H. Vali and K. A. Noghabi, *Colloid. Surface B.*, 2010, **81**, 397-  
406 405.
- 407
- 408
- 409
- 410
- 411
- 412
- 413
- 414

415 **Figure captions**

416 **Fig. 1** *Pseudomonas aeruginosa* cell growth (-●-) and rhamnolipid production (-○-) from pure  
417 cellobiose (-■-).

418 **Fig. 2** RSM plot showing the effect of FeSO<sub>4</sub> and NaNO<sub>3</sub> on rhamnolipid production.

419 **Fig. 3** RSM plot showing the effect of MgSO<sub>4</sub> and NaNO<sub>3</sub> on rhamnolipid production.

420 **Fig. 4** RSM plot showing the effect of MgSO<sub>4</sub> and FeSO<sub>4</sub> on rhamnolipid production.

421 **Fig. 5** *Pseudomonas aeruginosa* cell growth (--●-) and rhamnolipid production (-○-) from  
422 lignocellulosic hydrolysate at 30 °C for 72 h.

423 **Fig. 6** NMR spectrum of partially purified rhamnolipid sample.

424

425

426

427

428

429

430

431

432

433

434

435

436

437 **Table 1** Experimental design (conditions and responses) for rhamnolipid production from  
 438 lignocellulosic hydrolysate

Run order	MgSO <sub>4</sub> (ppm)	Na <sub>2</sub> PO <sub>4</sub> (ppm)	FeSO <sub>4</sub> (ppm)	NaNO <sub>3</sub> (ppm)	Rhamnolipid production (g/L)	
					Experimental	Predicted
1	143	5000	30	10000	7.9	7.926
2	333	5000	30	9000	9.15	9.136
3	143	9000	30	8000	8.30	8.358
4	333	9000	30	10000	7.95	7.998
5	143	5000	90	8000	8.55	8.447
6	333	5000	90	10000	8.2	8.087
7	143	9000	90	10000	8.0	7.952
8	333	9000	90	8000	8.6	8.519
9	333	5000	30	10000	7.70	7.695
10	143	9000	30	10000	7.75	7.631
11	333	9000	30	8000	8.60	8.598
12	143	5000	90	10000	8.40	8.47
13	333	5000	90	8000	7.75	7.937
14	143	9000	90	8000	8.35	8.43
15	333	9000	90	10000	8.10	8.168
16	143	7000	60	9000	9.30	9.334
17	333	7000	60	9000	9.35	9.263
18	238	5000	60	9000	8.70	8.652

19	238	9000	60	9000	8.8	8.795
20	238	7000	30	9000	7.20	7.207
21	238	7000	90	9000	7.50	7.44
22	238	7000	60	9000	7.84	7.909
23	238	7000	60	9000	7.90	7.909
24	238	7000	60	8000	6.80	6.661
25	238	7000	60	10000	6.30	6.373
26	238	7000	60	9000	7.90	7.909
27	238	7000	60	9000	7.85	7.909
28	238	7000	60	9000	7.95	7.909
29	238	7000	60	9000	7.85	7.909
30	238	7000	60	9000	7.84	7.909
31	238	7000	60	9000	7.96	7.909
32	238	7000	60	9000	7.92	7.909

---

439

440

441

442

443

444

445

446

447 **Table 2** ANOVA analysis of RSM model for rhamnolipid production from lignocellulosic  
 448 hydrolysate

Source	DF <sup>a</sup>	Seq SS <sup>b</sup>	Adj SS <sup>b</sup>	Adj MS <sup>c</sup>	F	P
Regression	14	12.6602	12.6602	0.9043	93.54	<0.001
Linear	4	0.545	8.2662	2.06655	213.75	<0.001
Square	4	11.4148	11.4777	2.86942	296.8	<0.001
Interaction	6	0.7004	0.7004	0.11673	12.07	<0.001
Residual Error	17	0.1644	0.1644	0.00967		
Lack-of-Fit	9	0.1466	0.1466	0.01628	7.32	0.005
Pure Error	8	0.0178	0.0178	0.00223		
Total	32	12.8246				
R <sup>2</sup>	98.72%	97.66%				

449 <sup>a</sup>: Degree of freedom

450 <sup>b</sup>: Sum of square

451 <sup>c</sup>: Mean square

452

453

454

455

456

457

458

459

460 **Table 3** Assignment of FTIR bands to different groups present in the rhamnolipid sample

(Wavenumber, $\text{cm}^{-1}$ )	Finger Print	Product Mixture containing Mono- & Di-Rhamnolipids
3300 - 3500	-OH due to water/moisture	Broad band at $\sim 3500 \text{ cm}^{-1}$
2850-3000	Aliphatic C-C and C-H bond stretching.	2926, 2854 $\text{cm}^{-1}$ : Symmetric and Asymmetric Stretching of C-C and C-H bonds.
1710-1760	Carboxylic Acid/Ester	1757 $\text{cm}^{-1}$ : -RCOO-
1500-1350	Bending vibrations of OH in Carboxylic acid	1456-1374 $\text{cm}^{-1}$
$\sim 1200$	C-C stretching	1244 $\text{cm}^{-1}$
$\sim 1000$	C-O Stretching	1097; 1050 $\text{cm}^{-1}$
$\sim 900-950$ ; 830-850	-O-C- (ring)	$\sim 910 \text{ cm}^{-1}$ ; 847 $\text{cm}^{-1}$

461

462

463

464

465

466

467

468

469

470

471

472

473 **Table 4**  $^1\text{H}$  NMR peak assignments to the partially purified product obtained from  
 474 rhamnolipid sample. The assignments are based on previous literature<sup>31</sup>

Functional group	Chemical shift (ppm) Assignment based on previous literature <sup>31</sup>	
	Mono Rhamnolipid	Di Rhamnolipid
-CH <sub>3</sub> (terminal)	0.879-0.939	0.862 and lower
-CH <sub>3</sub> (ring)	1.255 – 1.37	1.21 (small)
-(CH <sub>2</sub> ) <sub>n</sub> -	1.255 – 1.37	1.21 (small)
-CH <sub>2</sub> -COO-	2.41, 2.671 - 2.772	2 - 2.079, 2.31-2.334
4'-H	3.457	3.312
2', 3', 5'- H	3.605 – 3.65	3.727 - 3.78
1' - H	4.204 - 4.261	4.148 – 4.176
-O-CH-	4.714	4.907-5.013
-COO-CH-	5.345-5.37	Traces
-CH <sub>2</sub> CH-	7.21-7.718	7.21-7.29

475

476

477

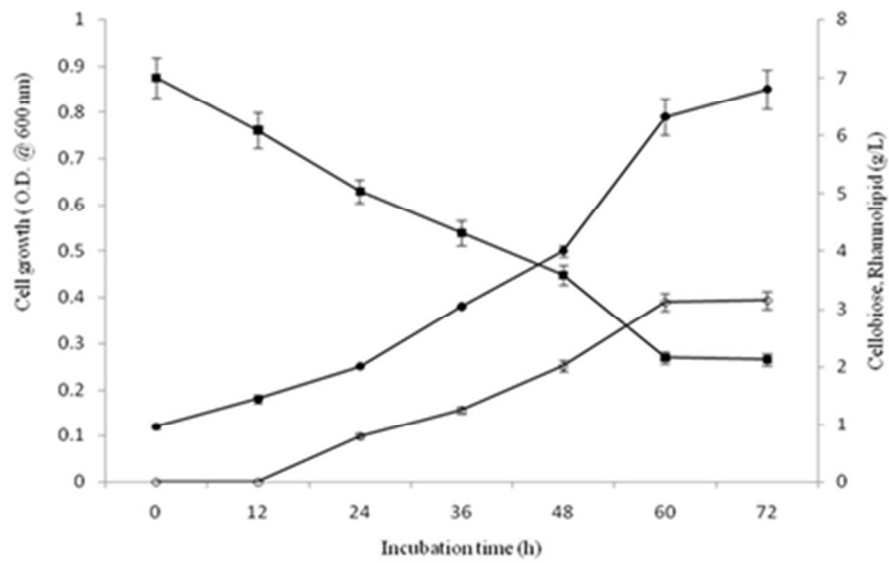


Fig. 1

38x27mm (300 x 300 DPI)

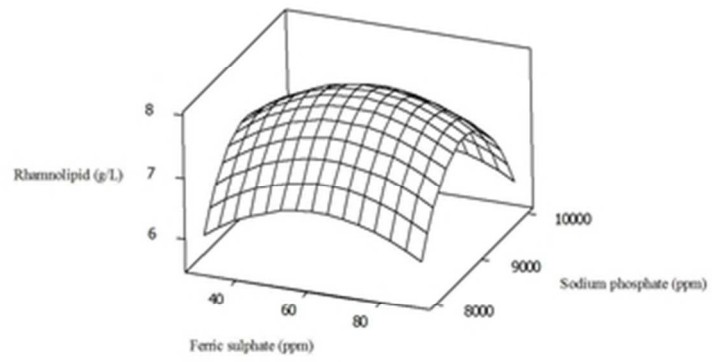
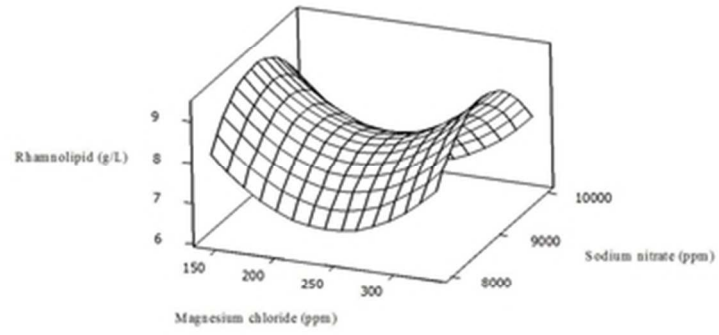


Fig. 2

34x20mm (300 x 300 DPI)

**Fig. 3**

33x20mm (300 x 300 DPI)

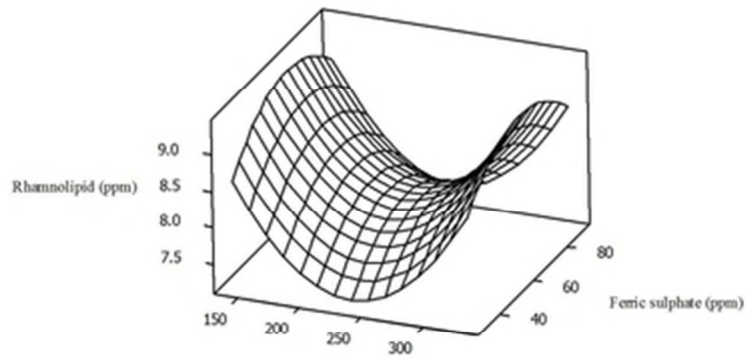


Fig. 4

34x20mm (300 x 300 DPI)

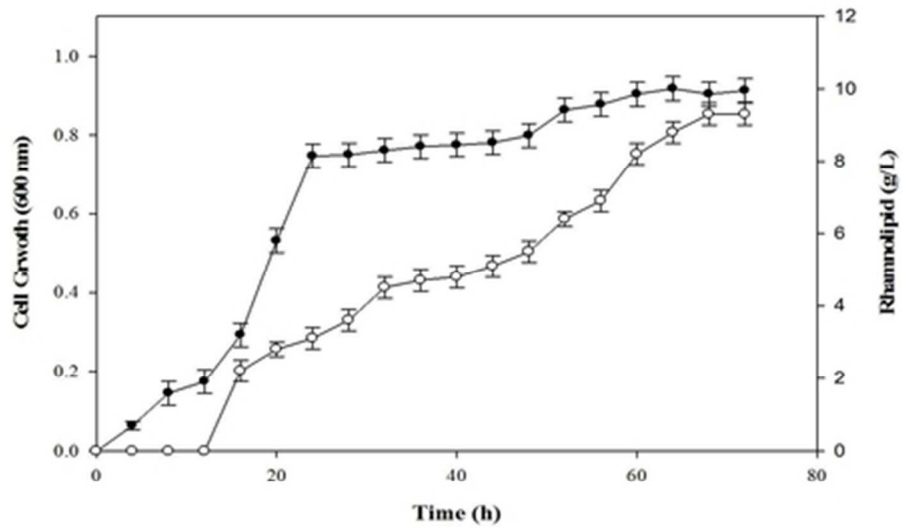


Fig. 5

38x26mm (300 x 300 DPI)

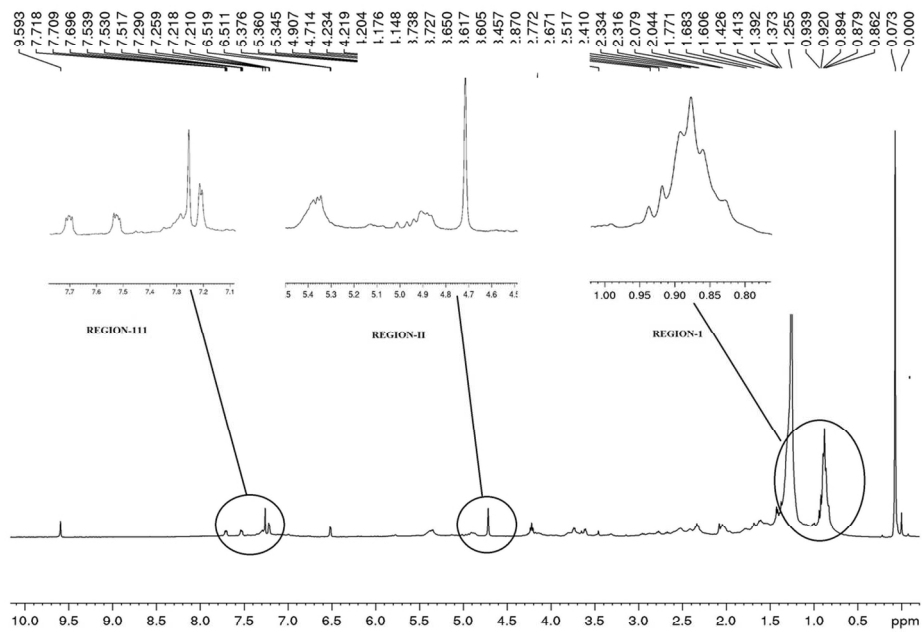


Fig. 6

110x85mm (300 x 300 DPI)